

# Transverse momentum resummation at N<sup>3</sup>LL+NNLO for diboson processes

JOHN M. CAMPBELL<sup>1</sup>, R. KEITH ELLIS<sup>2</sup>, TOBIAS NEUMANN<sup>3</sup>, AND SATYAJIT SETH<sup>4</sup><sup>1</sup>*Fermilab, PO Box 500, Batavia IL 60510-5011, USA*<sup>2</sup>*Institute for Particle Physics Phenomenology, Durham University, Durham, DH1 3LE, UK*<sup>3</sup>*Department of Physics, Brookhaven National Laboratory, Upton, New York 11973, USA*<sup>4</sup>*Physical Research Laboratory, Navrangpura, Ahmedabad - 380009, India,*

## Abstract

Diboson processes are one of the most accessible and stringent probes of the Standard Model's electroweak gauge structure at the LHC. They will be probed at the percent level at the high-luminosity LHC, challenging current theory predictions. We present transverse momentum resummed calculations at N<sup>3</sup>LL+NNLO for the processes  $ZZ$ ,  $WZ$ ,  $WH$  and  $ZH$ , compare our predictions with most recent LHC data and present predictions at 13.6 TeV including theory uncertainty estimates. For  $W^+W^-$  production we further present jet-veto resummed results at N<sup>3</sup>LL<sub>p</sub>+NNLO. Our calculations will be made publicly available in the upcoming MCFM release and allow future analyses to take advantage of improved predictions.

## Contents

<b>1</b>	<b>Introduction</b>	<b>1</b>
<b>2</b>	<b>Phenomenology</b>	<b>3</b>
2.1	$ZZ$ production . . . . .	3
2.1.1	$ZZ$ production at $\sqrt{s} = 13.6$ TeV . . . . .	3
2.1.2	Comparison with CMS measurements . . . . .	4
2.1.3	Comparison with ATLAS measurements . . . . .	5
2.2	$W^\pm Z$ production . . . . .	6
2.2.1	$WZ$ production at $\sqrt{s} = 13.6$ TeV . . . . .	6
2.2.2	Comparison with CMS measurements . . . . .	6
2.3	$W^+W^-$ production . . . . .	7
2.4	$WH$ and $ZH$ production . . . . .	8
<b>3</b>	<b>Conclusions</b>	<b>8</b>

## 1 Introduction

Large experimental efforts at the LHC are dedicated to the analysis of Standard Model (SM) electroweak gauge bosons. The production of  $\gamma$ ,  $W$ ,  $Z$  and  $H$  are typically considered either alone or in pairs, see table 1 for analyses of diboson processes at 13 TeV. Recent developments include evidence for the triboson processes [1–3]. The standard treatment of all these processes exploits the collinear factorization theorem to combine parton distribution functions (PDFs) and a hard scattering cross-section evaluated at a scale close to  $Q$  to derive a prediction. The scale  $Q$  is the invariant mass of the produced colorless final state. These collinear factoriza-

tion predictions are not appropriate at small transverse momentum  $q_T$ , where predictions at a fixed order of  $\alpha_s$  contain powers of  $L = \log(Q^2/q_T^2)$ . In addition, for the same reason, collinear factorization predictions are not suitable for cross-sections where jet activity is vetoed. In the region of small transverse momentum the fixed-order predictions need to be enhanced with resummation of these logarithms to all orders in  $\alpha_s$ . This necessitates an improved power counting where  $\log(Q^2/q_T^2) \sim 1/\alpha_s$  and exploits a factorization theorem at small  $q_T$ , valid up to terms suppressed by some power of  $q_T/Q$ .

Since the dominant fraction of cross-section resides at low transverse momentum, accurate theoretical con-

trol of this region is important. In addition, precise resummed predictions are necessary to validate the transverse-momentum spectra obtained from parton shower event generators operating at a lower logarithmic accuracy. Compared to single boson production, resummation effects for boson pair processes are expected to be even more important at the same value of  $q_T$  because the value of  $Q$  is much larger.

Of all massive diboson processes, the production of  $W^+W^-$  has received most theoretical and phenomenological attention. This is because of its sizable cross-section and its role as a background to top-quark production and to Higgs-boson production. Transverse momentum resummation in  $W^+W^-$  processes has been considered in refs. [4–7]. In particular ref. [7] discusses the resummation of transverse momentum logarithms at  $N^2LL+NNLO$ . The important topic of the resummation of jet veto logarithms in  $W^+W^-$  processes has been considered in refs. [7–10].

As for the other processes, ref. [11] considers the  $W^\pm Z$  and  $ZZ$  processes (as well as  $W^+W^-$ ) at  $N^2LL+NLO$ . Resummation in the  $ZZ$  (and  $W^+W^-$ ) processes has been considered in ref. [12] at  $N^2LL+NNLO$ . The interface of RadISH resummation to the MATRIX program allows for  $N^3LL+NNLO$  resummation [7] of all diboson processes but no phenomenological results for the  $W^\pm Z$  and  $ZZ$  processes at this level have been published.

In this paper we present an upgrade of CuTe-MCFM [13] which implements the SCET-based  $q_T$  resummation formalism of refs. [14–17]. We describe the  $N^3LL$  resummation matching to the remaining diboson processes  $WW$ ,  $ZZ$  and  $WZ$  that have been recently implemented in MCFM at fixed order NNLO [18]. Our goal is to show these improvements and the phenomenological capabilities of our code, especially since the diboson calculations were previously only presented at a technical level in MCFM [18]. We present resummed results for the massive diboson processes  $W^+W^-$ ,  $W^\pm Z$ , and  $WH$ ,  $ZH$  at the level of  $N^3LL+NNLO$ , compare with data as far as currently available, and provide predictions for the current LHC energy of  $\sqrt{s} = 13.6$  TeV.

In addition to  $q_T$  resummation, resummation effects become important when we veto against jet activity, for example in  $W^+W^-$  production to reduce background from  $t\bar{t}$  production. Although a discussion of jet-veto

Table 1: Experimental publications for boson pair production at 13 TeV.

Process	ATLAS	CMS
$WZ$	[19]	[20–22]
$ZZ$	[23, 24]	[25]
$WW$	[26, 27]	[21, 28]
$WH/ZH$	[29, 30]	[31]

results is not the principal aim of our study, in view of its experimental importance we present the results of jet-veto resummation for the case of  $W^+W^-$  production. We leave a detailed analysis of jet-veto resummation of this and other processes for a future study.



In this paper we use the SCET-based “collinear anomaly”  $q_T$  resummation formalism introduced in refs. [14–16]. Formulations of  $q_T$  resummation that are fully performed in impact parameter space have the drawback that the transformation from the impact parameter space  $x_T$  back to  $q_T$  involve the running coupling at scale  $x_T$ . Therefore, when performing the Fourier transform over all values of the impact parameter, one is forced to introduce a prescription to avoid the Landau pole in the running coupling. In the formulation of refs. [14–16] this issue is avoided, setting the scale directly in  $q_T$  space. The cross-section is obtained by combining the contributions from the partonic channels  $i, j \in q, \bar{q}, g$ . Up to terms suppressed by powers of  $q_T/Q$ , these channels exhibit a factorized form that is fully differential in the momenta  $\{q\}$  of the colorless final state

$$\begin{aligned}
 d\sigma_{ij}(p_1, p_2, \{q\}) = & \int_0^1 dz_1 \int_0^1 dz_2 d\sigma_{ij}^0(z_1 p_1, z_2 p_2, \{q\}) \mathcal{H}_{ij}(z_1 p_1, z_2 p_2, \{q\}, \mu) \\
 & \times \frac{1}{4\pi} \int d^2 x_\perp e^{-iq_\perp x_\perp} \left( \frac{x_T^2 Q^2}{b_0^2} \right)^{-F_{ij}(x_\perp, \mu)} \\
 & \times B_i(z_1, x_\perp, \mu) \cdot B_j(z_2, x_\perp, \mu), \quad (1)
 \end{aligned}$$

where  $p_1$  and  $p_2$  are the incoming hadron momenta. The function  $d\sigma_{ij}^0$  denotes the differential cross-section for the hard Born-level process and the hard-function  $\mathcal{H}_{ij}$  contains the associated virtual corrections. The beam functions  $B_i$  and  $B_j$  include the effects of soft and

collinear emissions at large transverse separation  $x_\perp$  and the indices  $i$  and  $j$  and the momentum fractions  $z_1$  and  $z_2$  refer to the partons which enter the hard process after these emissions. The collinear anomaly leads to the  $Q^2$ -dependent factor within the Fourier-integral over the transverse position  $x_\perp$ . The perturbatively calculable anomaly exponent  $F_{ij}$  is also referred to as the rapidity anomalous dimension in the framework of ref. [32]. We further have  $b_0 = 2e^{-\gamma_E}$ , where  $\gamma_E$  is the Euler constant, and  $x_T^2 = -x_\perp^2$ .

This framework for  $q_T$  resummation has been implemented at N<sup>3</sup>LL in CuTe-MCFM [13, 33], see ref. [13] for further details. Matching to large- $q_T$  fixed-order predictions were previously performed at relative order  $\alpha_s^2$  for the processes  $H, Z, W^\pm$  [34],  $W^\pm H$  and  $ZH$  [35],  $\gamma\gamma$  [36],  $Z\gamma$  [37], as well as at N<sup>4</sup>LL+N<sup>3</sup>LO for  $Z$  production in ref. [38]. The code is fully differential in the Born kinematics, including the decays of the bosons and provides an efficient way to estimate uncertainties from fixed-order truncation, resummation, and parton distribution functions.

To provide phenomenologically meaningful results also for  $W^+W^-$  production, we have implemented jet-veto resummation at N<sup>3</sup>LL<sub>p</sub>+NNLO following the collinear anomaly formalism of ref. [39]. Beam- and soft-functions are taken from refs. [40, 41] and the rapidity anomalous dimension at the two-loop level is taken from refs. [39, 42]. The notation N<sup>3</sup>LL<sub>p</sub> indicates that full N<sup>3</sup>LL accuracy is not achieved since an approximate form, valid at small jet-radii, for the three-loop term in the collinear anomaly exponent is used [43]. A detailed presentation of our implementation and its phenomenology for various processes will be presented elsewhere [44].

## 2 Phenomenology

In the following we first present finely binned transverse momentum spectra at 13.6 TeV and compare fixed-order and resummation improved predictions for each diboson process. These demonstrate the impact of the N<sup>3</sup>LL resummation for future analyses. In practice, in current experimental analyses the binning is still large, so that the impact of resummation is less apparent. We compare with experimental measurements as far as available for the 13 TeV LHC.

Table 2: Fiducial volume of the CMS  $ZZ$  analysis presented in ref. [25].

lepton cuts	$q_T^{l1} > 20 \text{ GeV}, q_T^{l2} > 10 \text{ GeV},$
	$q_T^{l3,4} > 10 \text{ GeV},  \eta^l  < 2.5$
lepton pair mass	$60 \text{ GeV} < m_{l-l^+} < 120 \text{ GeV}$

In section 2.1 we first consider  $ZZ$  production. For this process the transverse momentum of the vector boson pair system is directly measured, unlike for processes with  $W$  bosons which have missing energy. We compare with differential and total cross-section measurements from both CMS and ATLAS. We then present results for  $W^\pm Z$  production in section 2.2 and compare with ATLAS data. Finally we present jet-veto resummed predictions for  $W^+W^-$  in section 2.3 and compare to CMS measurements. Finally, we show differential predictions at 13.6 TeV for  $W^\pm H$  and  $ZH$  in section 2.4.

**Input parameters.** Throughout this paper we use the PDF set NNPDF31\_nnlo\_as\_0118 which has five active flavors, except for the  $W^+W^-$  process where we use the PDF set NNPDF31\_nnlo\_as\_0118\_nf\_4 with four active flavors [45]. We work in the electroweak  $G_\mu$  scheme with  $m_W = 80.385 \text{ GeV}$ ,  $m_Z = 91.1876 \text{ GeV}$ ,  $G_\mu = 1.166390 \times 10^{-5} \text{ GeV}^{-2}$  and further have  $\Gamma_W = 2.0854 \text{ GeV}$ ,  $\Gamma_Z = 2.4952 \text{ GeV}$ ,  $m_H = 125 \text{ GeV}$ ,  $m_t = 173.3 \text{ GeV}$ .

At fixed order we set the default renormalization and factorization scales to the invariant mass of the diboson system. For the resummation-improved results we vary hard scale, resummation scale and rapidity scale following refs. [13, 33]. We symmetrize resummation uncertainty bands to account for a frozen out downwards scale variation at small  $q_T$  that would otherwise evaluate  $\alpha_s$  in the non-perturbative regime. Since our resummation includes the matching through a transition function, we vary this function to estimate a matching uncertainty and include this in the uncertainty bands. For the detailed procedure we refer the reader to ref. [13].

### 2.1 $ZZ$ production

#### 2.1.1 $ZZ$ production at $\sqrt{s} = 13.6 \text{ TeV}$

We first present results for  $ZZ$  production at  $\sqrt{s} = 13.6 \text{ TeV}$  using the CMS cuts in table 2 [25] to study

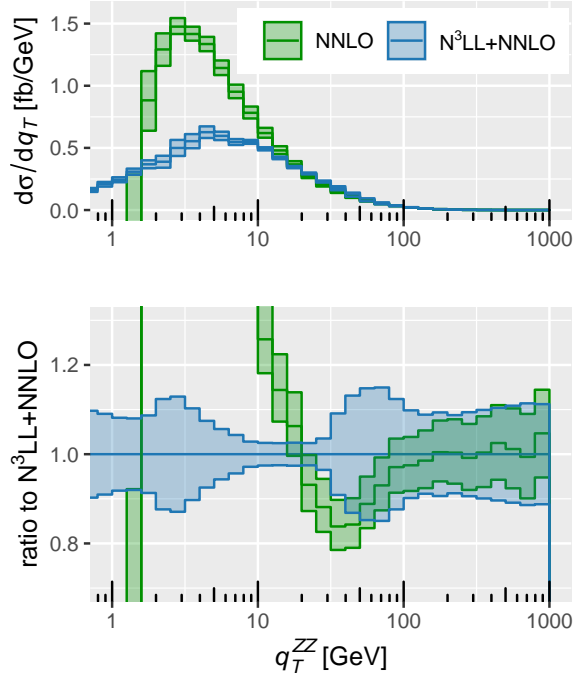


Figure 1: Transverse momentum distribution of the  $ZZ$  pair at NNLO and  $N^3LL+NNLO$  using the CMS cuts in table 2 [25], but at 13.6 TeV.

the impact of the resummation compared to fixed order. In fig. 1 we show the  $ZZ$  transverse momentum distribution at NNLO fixed-order and matched with  $N^3LL$  resummation. The transition region is around 30 GeV to 100 GeV and leads to uncertainties of about 15% in that region, comparable to the fixed-order uncertainties of 10%. The uncertainties in the resummation region for smaller  $q_T$  benefit from the high logarithmic accuracy until very small  $q_T$  of about 4 GeV to 5 GeV. Here resummation at the level of  $N^4LL$  would improve uncertainties further [38]. Overall we conclude that resummation within current theory uncertainty levels becomes important below about 50 GeV to 100 GeV.

### 2.1.2 Comparison with CMS measurements

We compare our predictions with the  $\sqrt{s} = 13$  TeV CMS results of ref. [25]. The cuts for our analysis are shown in table 2. To simplify our theoretical analysis we perform our calculations for  $Z$  bosons decaying to different-flavor leptons and account for all combinations with an overall factor of two. We have checked that this results in a negligible difference in our results at NLO. We neglect

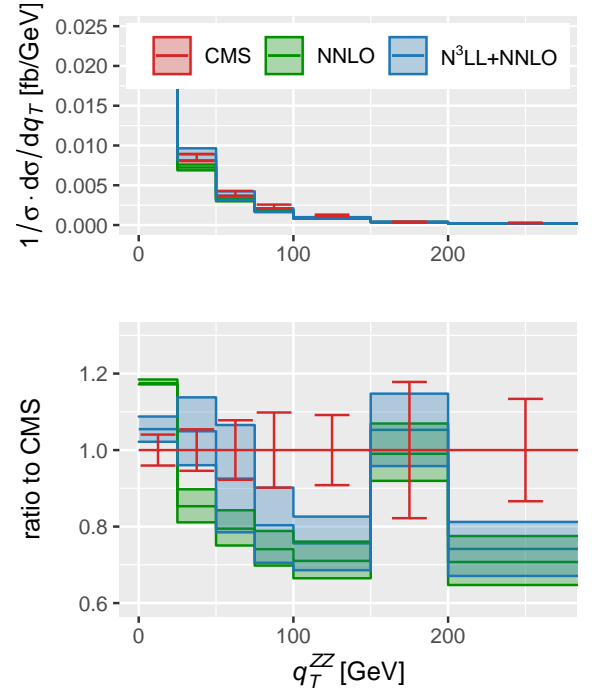


Figure 2: The  $q_T^{ZZ}$  distribution at NNLO and  $N^3LL+NNLO$  compared to the CMS data from ref. [25].

identical-particle effects (i.e. the  $e^-e^+e^-e^+$  final state is treated in the same way as  $e^-e^+\mu^-\mu^+$ ).

A comparison of the fixed-order NNLO and resummed  $N^3LL+NNLO$  predictions for  $q_T^{ZZ}$  is shown in fig. 2, also compared with the corresponding CMS data (c.f. Fig. 5 (left) of ref. [25]). The resummation improves the description of the experimental data up to 75 GeV noticeably, as anticipated by our finely binned analysis in fig. 1.

The CMS collaboration also presents a measurement of the transverse momentum of all four leptons, see fig. 4 (left) of ref. [25]. Our NNLO and  $N^3LL+NNLO$  results for this distribution are shown in fig. 3. In this distribution there is no evidence for the effects of resummation. Our theoretical study of the leading-lepton  $q_T^{l,1}$  spectrum shown in fig. 4 displays the importance of resummation effects, but only at very small  $q_T$  with large uncertainties. We have checked that the distributions of the other leptons are not significantly changed by  $q_T$  resummation, which leads to this effect being washed out in the experimental measurement.

Last, we compare the total fiducial cross-section predic-

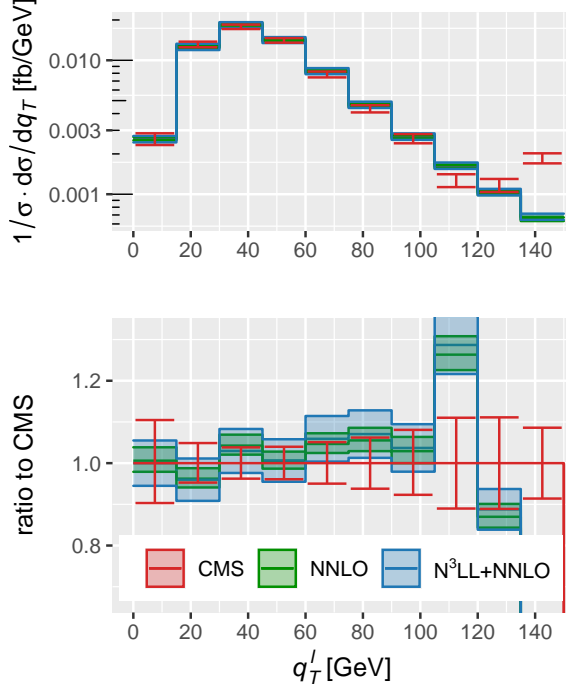


Figure 3: The  $q_T^l$  (summed over all leptons) distribution at NNLO and N<sup>3</sup>LL+NNLO, compared to the CMS data from ref. [25].

tion with the measurement in table 3 and find reasonable agreement between theory prediction and measurement.

### 2.1.3 Comparison with ATLAS measurements

We also compare with results from the ATLAS collaboration [24] using the cuts shown in table 4. As before, we perform our calculations for  $Z$  bosons decaying to different-flavor leptons and account for all combinations with an overall factor of two.

Table 3: Comparison of total fiducial  $ZZ$  cross-section predictions at NNLO, N<sup>3</sup>LL+NNLO with the CMS analysis combining measurements from 2016, 2017 and 2018 [25]. Fiducial cuts are as in table 2.

	cross-section [fb]
NNLO	$37.8_{-0.4}^{+0.5}$ (scale)
N <sup>3</sup> LL+NNLO	$36.0 \pm 0.8$ (scale) $\pm 0.8$ (match)
measurement	$40.5 \pm 0.7$ (sta.) $\pm 1.1$ (sys.) $\pm 0.7$ (lum.)

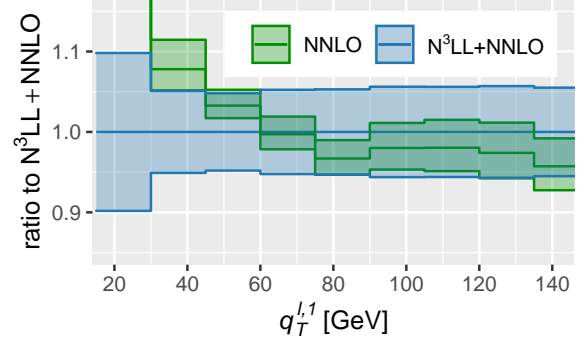


Figure 4: The  $q_T^{\ell_1}$  distribution at NNLO as a ratio to N<sup>3</sup>LL+NNLO. See fig. 3 for the sum of all leptons compared to CMS data.

Table 4: Setup for the ATLAS  $ZZ$  analysis at  $\sqrt{s} = 13$  TeV presented in ref. [24].

lepton cuts	$q_T^{\ell_1} > 20$ GeV, $q_T^{\ell_2} > 10$ GeV, $q_T^{\ell_{3,4}} > 5$ GeV, $q_T^e > 7$ GeV, $ \eta^\mu  < 2.7$ , $ \eta^e  < 2.47$
lepton separation	$\Delta R(\ell, \ell') > 0.05$

The ATLAS collaboration has performed measurements of the  $m_{4\ell}$  distribution in five slices of  $q_T^{4\ell}$  in fig. 15 of ref. [24]. We limit our comparison to the region  $m_{4\ell} > 182$  GeV to avoid the low invariant mass region populated by  $gg \rightarrow H$ . Since we are resumming logarithms  $\log(m_{4\ell}/q_T^{4\ell})$  our expectation is that the resummation should improve the agreement with data in the region of small  $q_T^{4\ell}$ , in particular as  $m_{4\ell}$  increases. We show results at NNLO and N<sup>3</sup>LL+NNLO in fig. 5 and indeed find this expectation to be correct. For brevity we only show the comparison with the first slice  $q_T^{4\ell} < 10$  GeV.

Table 5: Comparison of total fiducial  $ZZ$  cross-section predictions in the on-shell region  $180$  GeV  $< m_{4\ell} < 2000$  GeV at NNLO, N<sup>3</sup>LL+NNLO with the ATLAS analysis [24]. Fiducial cuts are as in table 4.

	cross-section [fb]
NNLO	$45.3_{-0.9}^{+1.1}$ fb
N <sup>3</sup> LL+NNLO	$43.7 \pm 0.7$ (scale) $\pm 0.8$ (match)
measurement	$49.3 \pm 0.8$ (sta.) $\pm 0.8$ (sys.) $\pm 0.8$ (lum.)

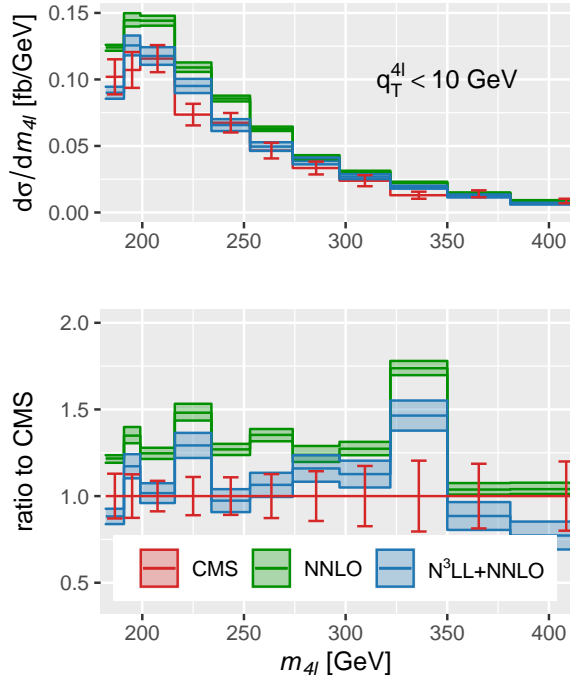


Figure 5: The  $m_{4l}$  distribution for  $q_T^{4l} < 10$  GeV at NNLO and N<sup>3</sup>LL+NNLO compared with ATLAS data from ref. [24].

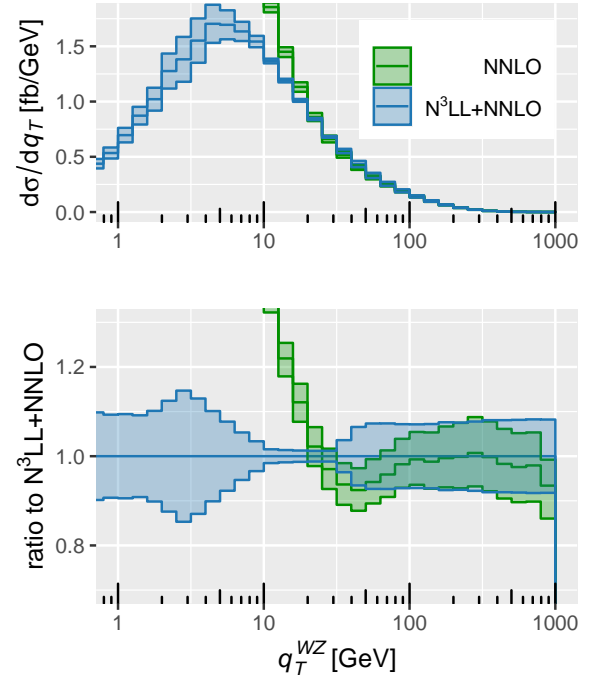


Figure 6: Comparison of NNLO and N<sup>3</sup>LL+NNLO predictions for truth  $p_T^{W^\pm Z}$  at 13.6 TeV using the CMS cuts in table 6.

## 2.2 $W^\pm Z$ production

### 2.2.1 $WZ$ production at $\sqrt{s} = 13.6$ TeV

We begin with predictions at 13.6 TeV for run 3 of the LHC using CMS cuts as in table 6.

Fig. 6 illustrates the impact that resummation has on the  $q_T$  distribution. For the purposes of illustration,  $q_T$  is constructed from the full  $WZ$  four-vector, although of course this is not a quantity that can be directly measured in experiment. Similar to the other diboson processes, the resummation becomes essential below 50 GeV to 100 GeV.

A related quantity, which is often measured in experiment, is the transverse mass of the  $WZ$  system,  $m_T^{WZ}$ , which following ref. [19] is defined as,

$$(m_T^{WZ})^2 = \left( \sum_{\ell=1}^3 p_T^\ell + E_T^{\text{miss}} \right)^2 - \left[ \left( \sum_{\ell=1}^3 p_x^\ell + E_x^{\text{miss}} \right)^2 + \left( \sum_{\ell=1}^3 p_y^\ell + E_y^{\text{miss}} \right)^2 \right]. \quad (2)$$

The predictions for this variable are shown in fig. 7. At the current level of theory uncertainties, resummation effects are relevant for transverse masses less than about 100 GeV, far below the peak region.

### 2.2.2 Comparison with CMS measurements

For  $W^\pm Z$  production, we choose to focus on the CMS analysis of ref. [22]. The parameters and cuts for this study are given in table 6. As in previous sections, we slightly simplify the theoretical analysis by computing the cross-section for different-flavor leptons only. We sum over lepton flavors by applying an overall factor of four, neglecting same-flavor effects at the 2% level [22] that are, however, unimportant for the current experimental and theoretical accuracy. We first compare total fiducial cross-sections in table 7 and find agreement between theory prediction and measurement within uncertainties.

We now turn to the differential comparison with the measurement of ref. [22]. The transverse momentum distribution of the lepton in the  $W$  decay (summed over both  $W$  charges)  $q_T^{\ell W}$  is shown at NNLO and N<sup>3</sup>LL+NNLO

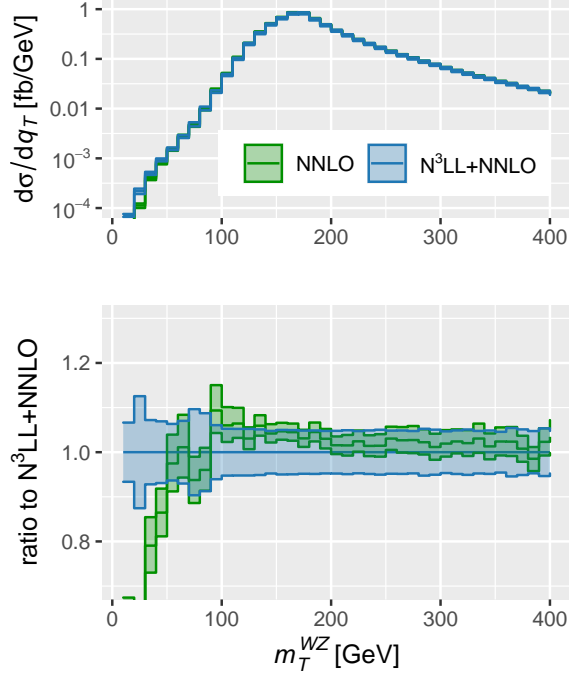


Figure 7: Comparison of NNLO and  $N^3\text{LL}+\text{NNLO}$  predictions for the truth  $m_T^{W^\pm Z}$  at 13.6 TeV using the CMS cuts in table 6.

Table 6: Setup for the CMS  $WZ$  fiducial volume analysis at  $\sqrt{s} = 13$  TeV presented in ref. [22].

$$\text{lepton cuts} \left\{ \begin{array}{l} p_T^{\ell Z_1} > 25 \text{ GeV}, p_T^{\ell Z_2} > 10 \text{ GeV}, \\ p_T^{\ell W} > 25 \text{ GeV}, |\eta^\ell| < 2.5, \\ 60 \text{ GeV} < m_{\ell-\ell^+} < 120 \text{ GeV}, \\ M(\ell_{Z_1}, \ell_{Z_2}, \ell_W) > 100 \text{ GeV} \end{array} \right.$$

in fig. 8. Resummation appears to have no significant effect for this variable.

### 2.3 $W^+W^-$ production

The experimental study of  $W^+W^-$  production is subject to large backgrounds, principally from top production, but also from Drell-Yan processes,  $W$ +jet production, and other di- and tri-boson production processes. Reducing the background from top production to an acceptable level currently requires the imposition of a veto on jet activity. We have implemented jet-veto resummation for all single boson and boson pair processes at the level of  $N^3\text{LL}_p+\text{NNLO}$  based on the collinear anomaly formalism [39] and the ingredients available in the liter-

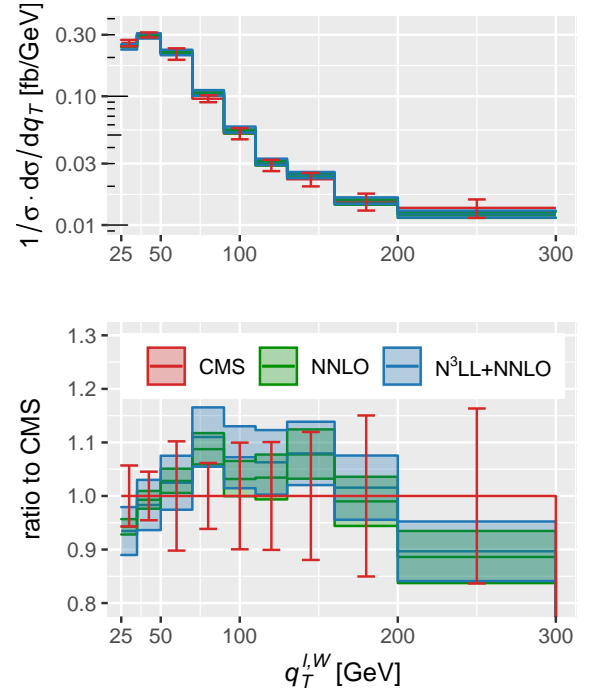


Figure 8: The  $q_T^{\ell W}$  distribution for  $W^\pm Z$  at NNLO and  $N^3\text{LL}+\text{NNLO}$  compared to the CMS data from ref. [22].

ature [40, 41]. Here we only present results for  $W^+W^-$  production and leave a detailed jet-veto study for a future publication [44]. Previous detailed analyses of this process in the literature are at the level of  $N^2\text{LL}$  [7, 8, 10] and  $N^3\text{LL}_p+\text{NNLO}$  [9]. Our implementation of the jet veto resummation is closer to full  $N^3\text{LL}+\text{NNLO}$  than ref. [9], since it contains complete results for the beam function [41], including dependence on the jet radius  $R$ .

In fig. 9 we present jet-veto resummed results at  $\sqrt{s} = 13$  TeV using the CMS cuts in table 8 compared with the corresponding analysis [28]. The calculation is performed using the  $n_f = 4$  version of the PDFs to ensure consistency across the entire calculation. We include a factor of 4 in our results to account for the sum over both electrons and muons, neglecting contributions from  $ZZ \rightarrow \ell\bar{\ell}\nu\bar{\nu}$  that are negligible as long as a suitable cut on  $|m_{\ell\bar{\ell}} - m_Z|$  is applied. We include the  $gg$  channel at leading fixed order. For simplicity we do not include a transition function for this calculation but perform a naive matching. The cross-section is dominated by the resummed part, with 5 to 10 percent matching corrections between  $q_T^{\text{veto}} = 25$  GeV and 60 GeV. Overall

Table 7: Comparison of total fiducial  $WZ$  cross-section predictions at NNLO, N<sup>3</sup>LL+NNLO with the CMS analysis [22]. Fiducial cuts are as in table 6.

	$W^-Z \rightarrow e^- \bar{\nu} \mu^- \mu^+$	$W^+Z \rightarrow e^+ \nu \mu^- \mu^+$
NNLO	$29.9^{+0.7}_{-0.6}$	$42.8^{+0.9}_{-0.9}$
N <sup>3</sup> LL+NNLO	$29.0 \pm 1.1$ (scale) $\pm 0.3$ (match.)	$41.6 \pm 1.5$ (scale) $\pm 0.4$ (match.)
measurement	$31.8 \pm 1.4$ (sta.) $\pm 1.1$ (sys.) $\pm 0.6$ (lum.)	$43.1 \pm 1.4$ (sta.) $\pm 1.5$ (sys.) $\pm 0.9$ (lum.)

Table 8: Setup for the CMS  $W^+W^-$  fiducial volume analysis at  $\sqrt{s} = 13$  TeV presented in ref. [28].

lepton cuts	$q_T^\ell > 20$ GeV, $ \eta^\ell  < 2.5$ , $m_{\ell\ell} > 20$ GeV, $q_T^{\ell\ell} > 30$ GeV, $q_T^{\text{miss}} > 30$ GeV
jet veto	anti- $k_T$ , $R = 0.4$ , 0-jet events only

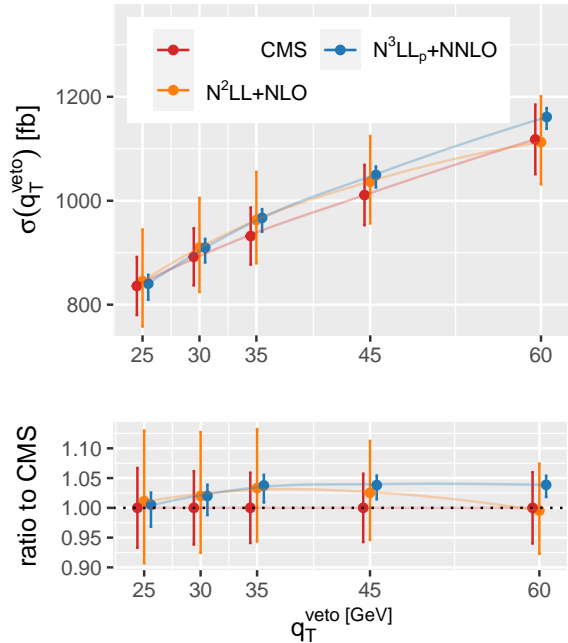


Figure 9: Jet-veto resummed cross-sections for  $W^+W^- \rightarrow 2e2\nu$  production at 13 TeV using the CMS cuts in table 8 of this section in comparison with the CMS measurement [28]. The solid lines are interpolations to guide the eye.

there is agreement between our theory predictions and the measurements within uncertainties.

## 2.4 $WH$ and $ZH$ production

Matched N<sup>3</sup>LL+NNLO calculations for  $WH$  and  $ZH$  were implemented in ref. [13], but no results were presented. Here we present predictions for these two processes at  $\sqrt{s} = 13.6$  TeV to demonstrate the capabilities of the code. For this demonstration we do not apply cuts on the electroweak final state after  $W$ ,  $Z$  and  $H$  bosons decay. We further divide out the branching ratio to give the total rate independent of the particular decay channel.

We have also upgraded our code to include resummation for  $W\gamma$  production, but do not show results, since  $Z\gamma$  has been extensively discussed in ref. [13]. In particular, the issue of photon isolation plays a big role in this process and requires a dedicated discussion.

## 3 Conclusions

The experimental study of massive diboson kinematics is still in its infancy. Currently only 5% of the final LHC luminosity has been recorded and the high-luminosity LHC will require precise predictions at the percent level. We have presented transverse momentum resummed results at the level of N<sup>3</sup>LL+NNLO for the production of pairs of vector bosons  $ZZ$ ,  $W^\pm Z$ ,  $W^\pm H$  and  $ZH$ . Where experimental data has been available in sufficient detail we have shown that the inclusion of the resummed logarithms leads to improved agreement with the data at low  $q_T$ . For  $W^+W^-$  production we have shown jet-veto resummed predictions in comparison with measurements and find agreement within uncertainties.

Current binning of experimental data is not fine-grained and still quite inclusive, in particular one often has a



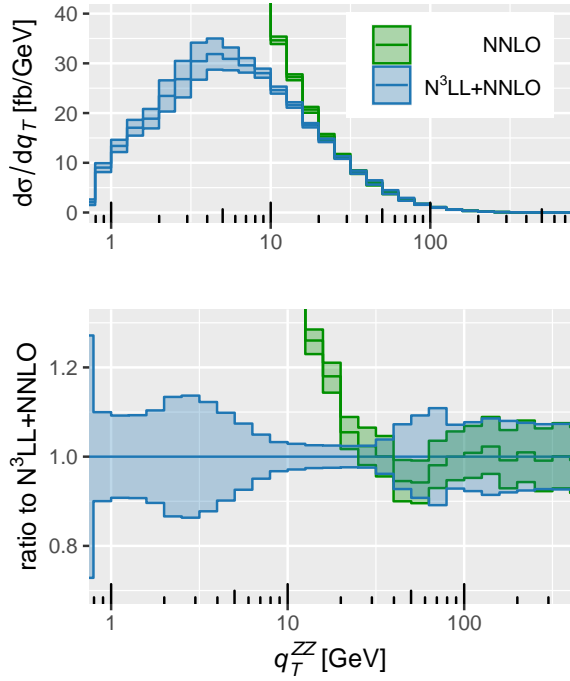


Figure 10: The  $q_T^{WH}$  distribution for  $W^+H + W^-H$  at N<sup>3</sup>LL+NNLO compared to fixed order NNLO.

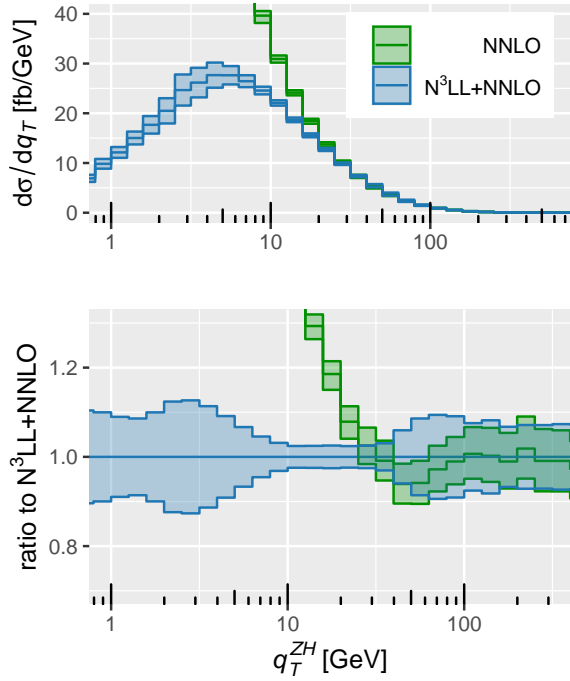


Figure 11: The  $q_T^{ZH}$  distribution at N<sup>3</sup>LL+NNLO compared to fixed order NNLO.

large first bin starting at  $q_T = 0$ . This diminishes the effect of  $q_T$  resummation, which is most necessary at the differential level at small  $q_T$ , but also for certain sets of fiducial cuts at an inclusive level at a sufficient level of precision [46]. Our more finely binned predictions for  $\sqrt{s} = 13.6$  TeV show the importance of resummation when precise enough data becomes available.

With decreasing experimental uncertainties it will be necessary to take into account NLO corrections to the  $gg$  channel [47, 48], which we only include at LO, as well as NLO electroweak corrections [49–51] that can be included by the use of automated one-loop tools [49, 52, 53]. Further refinements are possible through the inclusion of identical-particle effects, which we have neglected so far but are straightforward to include once experimental results become sufficiently precise.

Our calculation will be publicly available in the upcoming release of MCFM and can be used to reproduce the results in this study as well as to perform further studies with modified parameters. With this, our calculation also provides an important theoretical tool for comparison and tuning of approaches based on parton shower event generators operating at low logarithmic accuracy.

**Acknowledgements.** This manuscript has been authored by Fermi Research Alliance, LLC under Contract No. DE-AC02-07CH11359 with the U.S. Department of Energy, Office of Science, Office of High Energy Physics (JMC). TN is supported by the United States Department of Energy under Grant Contract DE-SC0012704. This research used resources of the National Energy Research Scientific Computing Center (NERSC), a U.S. Department of Energy Office of Science User Facility located at Lawrence Berkeley National Laboratory, operated under Contract No. DE-AC02-05CH11231 using NERSC award HEP-ERCAP0021890.

## References

- [1] CMS collaboration, *Observation of the Production of Three Massive Gauge Bosons at  $\sqrt{s} = 13$  TeV*, *Phys. Rev. Lett.* **125** (2020) 151802 [2006.11191].

- [2] CMS collaboration, *Search for the production of  $W^\pm W^\pm W^\mp$  events at  $\sqrt{s} = 13$  TeV*, *Phys. Rev. D* **100** (2019) 012004 [1905.04246].
- [3] ATLAS collaboration, *Evidence for the production of three massive vector bosons with the ATLAS detector*, *Phys. Lett. B* **798** (2019) 134913 [1903.10415].
- [4] M. Grazzini, *Soft-gluon effects in  $WW$  production at hadron colliders*, *JHEP* **01** (2006) 095 [hep-ph/0510337].
- [5] P. Meade, H. Ramani and M. Zeng, *Transverse momentum resummation effects in  $W^+W^-$  measurements*, *Phys. Rev. D* **90** (2014) 114006 [1407.4481].
- [6] W. Bizon, P.F. Monni, E. Re, L. Rottoli and P. Torrielli, *Momentum-space resummation for transverse observables and the Higgs  $p_\perp$  at  $N^3LL+NNLO$* , *JHEP* **02** (2018) 108 [1705.09127].
- [7] S. Kallweit, E. Re, L. Rottoli and M. Wiesemann, *Accurate single- and double-differential resummation of colour-singlet processes with MATRIX+RADISH:  $W^+W^-$  production at the LHC*, *JHEP* **12** (2020) 147 [2004.07720].
- [8] P. Jaiswal and T. Okui, *Explanation of the  $WW$  excess at the LHC by jet-veto resummation*, *Phys. Rev. D* **90** (2014) 073009 [1407.4537].
- [9] S. Dawson, P. Jaiswal, Y. Li, H. Ramani and M. Zeng, *Resummation of jet veto logarithms at  $N^3LL_a + NNLO$  for  $W^+W^-$  production at the LHC*, *Phys. Rev. D* **94** (2016) 114014 [1606.01034].
- [10] L. Arpino, A. Banfi, S. Jäger and N. Kauer, *BSM  $WW$  production with a jet veto*, *JHEP* **08** (2019) 076 [1905.06646].
- [11] Y. Wang, C.S. Li, Z.L. Liu, D.Y. Shao and H.T. Li, *Transverse-Momentum Resummation for Gauge Boson Pair Production at the Hadron Collider*, *Phys. Rev. D* **88** (2013) 114017 [1307.7520].
- [12] M. Grazzini, S. Kallweit, D. Rathlev and M. Wiesemann, *Transverse-momentum resummation for vector-boson pair production at  $NNLL+NNLO$* , *JHEP* **08** (2015) 154 [1507.02565].
- [13] T. Becher and T. Neumann, *Fiducial  $q_T$  resummation of color-singlet processes at  $N^3LL+NNLO$* , *JHEP* **03** (2021) 199 [2009.11437].
- [14] T. Becher and M. Neubert, *Drell-Yan Production at Small  $q_T$ , Transverse Parton Distributions and the Collinear Anomaly*, *Eur. Phys. J. C* **71** (2011) 1665 [1007.4005].
- [15] T. Becher, M. Neubert and D. Wilhelm, *Electroweak Gauge-Boson Production at Small  $q_T$ : Infrared Safety from the Collinear Anomaly*, *JHEP* **02** (2012) 124 [1109.6027].
- [16] T. Becher, M. Neubert and D. Wilhelm, *Higgs-Boson Production at Small Transverse Momentum*, *JHEP* **05** (2013) 110 [1212.2621].
- [17] T. Becher and M. Hager, *Event-Based Transverse Momentum Resummation*, *Eur. Phys. J. C* **79** (2019) 665 [1904.08325].
- [18] J.M. Campbell, R.K. Ellis and S. Seth, *Non-local slicing approaches for NNLO QCD in MCFM*, *JHEP* **06** (2022) 002 [2202.07738].
- [19] ATLAS collaboration, *Measurement of  $W^\pm Z$  production cross sections and gauge boson polarisation in  $pp$  collisions at  $\sqrt{s} = 13$  TeV with the ATLAS detector*, *Eur. Phys. J. C* **79** (2019) 535 [1902.05759].
- [20] CMS collaboration, *Measurements of the  $pp \rightarrow WZ$  inclusive and differential production cross section and constraints on charged anomalous triple gauge couplings at  $\sqrt{s} = 13$  TeV*, *JHEP* **04** (2019) 122 [1901.03428].
- [21] CMS collaboration, *Search for anomalous triple gauge couplings in  $WW$  and  $WZ$  production in lepton + jet events in proton-proton collisions at  $\sqrt{s} = 13$  TeV*, *JHEP* **12** (2019) 062 [1907.08354].
- [22] CMS collaboration, *Measurement of the inclusive and differential  $WZ$  production cross sections, polarization angles, and triple gauge couplings in  $pp$  collisions at  $\sqrt{s} = 13$  TeV*, 2110.11231.
- [23] ATLAS collaboration, *Measurement of  $ZZ$  production in the  $\ell\ell\nu\nu$  final state with the ATLAS*

- detector in  $pp$  collisions at  $\sqrt{s} = 13$  TeV, *JHEP* **10** (2019) 127 [1905.07163].
- [24] ATLAS collaboration, *Measurements of differential cross-sections in four-lepton events in 13 TeV proton-proton collisions with the ATLAS detector*, 2103.01918.
- [25] CMS collaboration, *Measurements of  $pp \rightarrow ZZ$  production cross sections and constraints on anomalous triple gauge couplings at  $\sqrt{s} = 13$  TeV*, *Eur. Phys. J. C* **81** (2021) 200 [2009.01186].
- [26] ATLAS collaboration, *Measurement of the  $W^+W^-$  production cross section in  $pp$  collisions at a centre-of-mass energy of  $\sqrt{s} = 13$  TeV with the ATLAS experiment*, *Phys. Lett. B* **773** (2017) 354 [1702.04519].
- [27] ATLAS collaboration, *Measurement of fiducial and differential  $W^+W^-$  production cross-sections at  $\sqrt{s} = 13$  TeV with the ATLAS detector*, *Eur. Phys. J. C* **79** (2019) 884 [1905.04242].
- [28] CMS collaboration,  *$W^+W^-$  boson pair production in proton-proton collisions at  $\sqrt{s} = 13$  TeV*, *Phys. Rev. D* **102** (2020) 092001 [2009.00119].
- [29] ATLAS collaboration, *Measurements of  $WH$  and  $ZH$  production in the  $H \rightarrow b\bar{b}$  decay channel in  $pp$  collisions at 13 TeV with the ATLAS detector*, *Eur. Phys. J. C* **81** (2021) 178 [2007.02873].
- [30] ATLAS collaboration, *Measurement of the associated production of a Higgs boson decaying into  $b$ -quarks with a vector boson at high transverse momentum in  $pp$  collisions at  $\sqrt{s} = 13$  TeV with the ATLAS detector*, *Phys. Lett. B* **816** (2021) 136204 [2008.02508].
- [31] CMS collaboration, *Observation of Higgs boson decay to bottom quarks*, *Phys. Rev. Lett.* **121** (2018) 121801 [1808.08242].
- [32] J.-Y. Chiu, A. Jain, D. Neill and I.Z. Rothstein, *A Formalism for the Systematic Treatment of Rapidity Logarithms in Quantum Field Theory*, *JHEP* **05** (2012) 084 [1202.0814].
- [33] T. Neumann, *The diphoton  $q_T$  spectrum at  $N^3LL' + NNLO$* , *Eur. Phys. J. C* **81** (2021) 905 [2107.12478].
- [34] R. Boughezal, J.M. Campbell, R.K. Ellis, C. Focke, W. Giele, X. Liu et al., *Color singlet production at NNLO in MCFM*, *Eur. Phys. J. C* **77** (2017) 7 [1605.08011].
- [35] J.M. Campbell, R.K. Ellis and C. Williams, *Associated production of a Higgs boson at NNLO*, *JHEP* **06** (2016) 179 [1601.00658].
- [36] J.M. Campbell, R.K. Ellis, Y. Li and C. Williams, *Predictions for diphoton production at the LHC through NNLO in QCD*, *JHEP* **07** (2016) 148 [1603.02663].
- [37] J.M. Campbell, T. Neumann and C. Williams,  *$Z\gamma$  Production at NNLO Including Anomalous Couplings*, *JHEP* **11** (2017) 150 [1708.02925].
- [38] T. Neumann and J. Campbell, *Fiducial Drell-Yan production at the LHC improved by transverse-momentum resummation at  $N^4LL+N^3LO$* , 2207.07056.
- [39] T. Becher, M. Neubert and L. Rothen, *Factorization and  $N^3LL_p+NNLO$  predictions for the Higgs cross section with a jet veto*, *JHEP* **10** (2013) 125 [1307.0025].
- [40] S. Abreu, J.R. Gaunt, P.F. Monni and R. Szafron, *The analytic two-loop soft function for leading-jet  $p_T$* , *JHEP* **08** (2022) 268 [2204.02987].
- [41] S. Abreu, J.R. Gaunt, P.F. Monni, L. Rottoli and R. Szafron, *Quark and gluon two-loop beam functions for leading-jet  $p_T$  and slicing at NNLO*, 2207.07037.
- [42] A. Banfi, P.F. Monni, G.P. Salam and G. Zanderighi, *Higgs and Z-boson production with a jet veto*, *Phys. Rev. Lett.* **109** (2012) 202001 [1206.4998].
- [43] A. Banfi, F. Caola, F.A. Dreyer, P.F. Monni, G.P. Salam, G. Zanderighi et al., *Jet-vetoed Higgs cross section in gluon fusion at  $N^3LO+NNLL$  with small- $R$  resummation*, *JHEP* **04** (2016) 049 [1511.02886].
- [44] J.M. Campbell, R.K. Ellis, T. Neumann and S. Seth, *In preparation*, .
- [45] NNPDF collaboration, *Parton distributions from high-precision collider data*, *Eur. Phys. J. C* **77** (2017) 663 [1706.00428].

- [46] G.P. Salam and E. Slade, *Cuts for two-body decays at colliders*, *JHEP* **11** (2021) 220 [2106.08329].
- [47] M. Grazzini, S. Kallweit, M. Wiesemann and J.Y. Yook,  *$W^+W^-$  production at the LHC: NLO QCD corrections to the loop-induced gluon fusion channel*, *Phys. Lett. B* **804** (2020) 135399 [2002.01877].
- [48] M. Grazzini, S. Kallweit, M. Wiesemann and J.Y. Yook,  *$ZZ$  production at the LHC: NLO QCD corrections to the loop-induced gluon fusion channel*, *JHEP* **03** (2019) 070 [1811.09593].
- [49] S. Kallweit, J.M. Lindert, P. Maierhöfer, S. Pozzorini and M. Schönherr, *NLO electroweak automation and precise predictions for  $W$ +multijet production at the LHC*, *JHEP* **04** (2015) 012 [1412.5157].
- [50] S. Kallweit, J.M. Lindert, S. Pozzorini and M. Schönherr, *NLO QCD+EW predictions for  $2\ell 2\nu$  diboson signatures at the LHC*, *JHEP* **11** (2017) 120 [1705.00598].
- [51] M. Grazzini, S. Kallweit, J.M. Lindert, S. Pozzorini and M. Wiesemann, *NNLO QCD + NLO EW with Matrix+OpenLoops: precise predictions for vector-boson pair production*, *JHEP* **02** (2020) 087 [1912.00068].
- [52] S. Actis, A. Denner, L. Hofer, J.-N. Lang, A. Scharf and S. Uccirati, *RECOLA: REcursive Computation of One-Loop Amplitudes*, *Comput. Phys. Commun.* **214** (2017) 140 [1605.01090].
- [53] M. Chiesa, N. Greiner and F. Tramontano, *Automation of electroweak corrections for LHC processes*, *J. Phys. G* **43** (2016) 013002 [1507.08579].